A Brief Evaluation of Precipitation from the North American Regional Reanalysis

Melissa S. Bukovsky

David J. Karoly

School of Meteorology, University of Oklahoma
Norman OK

Corresponding Author Address: Melissa S. Bukovsky, School of Meteorology, University of Oklahoma, 120 David L. Boren Blvd., Norman, OK 73072.

Email: mbukovsky@ou.edu

Submitted to:

Journal of Hydrometeorology

June 2006

Revised: September 2006

Revised: November 2006

Abstract

Several aspects of the precipitation climatology from the North American Regional Reanalysis (NARR) are analyzed and compared with two other reanalyses and one set of gridded observations over a domain encompassing the United States. The spatial distribution, diurnal cycle, and annual cycle of precipitation are explored to establish the reliability of the reanalyses and to judge their usefulness. While the NARR provides a much improved representation of precipitation over that of the other reanalyses examined, some inaccuracies are found and have been highlighted as a warning to potential users of the data.

I. Introduction

Many studies utilize the combination of observations and model assimilation and integration known as 'reanalysis' data as a benchmark for model comparison, while others employ it to create initial conditions for case studies or for regional climatology or hydrometeorological analysis (e.g. Hane et al. 2001, Betts 2004, Ruiz-Barradas and Nigam 2005). Reanalyses basically provide another data set for use in further understanding our environment. They are, however, only an estimate of the real state of the atmosphere. Using reanalysis data may inadvertently add inaccuracies to a study if the data are not used with caution, as they do not always match what is observed, particularly for precipitation (Higgins et al. 1996b, Betts et al. 1998, Kållberg et al. 2004, West et al. 2006). In this respect, precipitation reanalyses are in a different category relative to other available reanalysis variables. Identifying inaccuracies that reanalyses may contain is the first step towards correcting them. This study, therefore, aims to identify some strong and weak points in the precipitation field from the newly available North American Regional Reanalysis (NARR, Mesinger et al. 2006) and several other available reanalyses.

In general, qualitative similarities and differences between the different reanalyses are identified in terms of precipitation in the North American region. This study concentrates on the NARR precipitation climatology over a domain encompassing the United States with an emphasis on warm season precipitation during the 1990s. The spatial distribution, intensity, diurnal cycle, and annual cycle of precipitation are explored in order to establish the reliability of the reanalyses. The goal is to identify the usefulness of the NARR versus the other precipitation

datasets and to provide a warning to potential users about some of the inaccuracies the reanalyses may contain.

II. Reanalyses and Methods

Precipitation from three reanalyses and one objectively analyzed dataset are used in this study; their descriptions follow. The objectively analyzed dataset will be used to approximate the "truth". Unless otherwise noted, all results use the original horizontal resolution of the data. Interpolating reanalyses to matching grids does not change the qualitative results presented in the next section.

The National Center for Environmental Prediction (NCEP)/Department of Energy (DOE) Atmospheric Model Intercomparisson Project (AMIP-II) global reanalysis (NCEP-DOE (also known as R-2), Kanamitsu et al. 2002), the European Center for Medium-Range Weather Forecasts' global reanalysis (ERA-40, Kållberg et al. 2004), and NCEP's NARR (Mesinger et al. 2006) were chosen because of their widespread use and potential for application in verification and diagnostic studies. The Climate Prediction Center's hourly US objectively analyzed, gridded, observationally based precipitation dataset (hereafter referred to as CPC, Higgins et al. 1996a) was chosen for its time resolution, successful application in other studies (e.g. Trenberth 1998, Dai 1999), and full US coverage.

These reanalyses were originally gathered and compared for use in climate model verification, but interesting results were found during the comparison which motivated this note. As data from the models at a high temporal resolution are only available from 1991-2000, that decade was used in the verification and will also be used for this study. Where precipitation rate

data is referred to as being hourly, three-hourly, or six-hourly, it has been averaged over that span of time, starting at a given hour (e.g. a value at 0300 UTC from three-hourly data would be the average precipitation rate from 0300 – 0600 UTC).

a. NCEP-DOE

The NCEP-DOE is an updated version of the NCEP/NCAR (National Center for Atmospheric Research) global reanalysis (NCEP-GR, Kalnay et al. 1996). The assimilation system that produces the NCEP-DOE is an improved version of the system that created the NCEP-GR. It utilizes a version of the NCEP global spectral model. The horizontal resolution is approximately 209-km (T62) and there are 28 vertical levels. Parameterizations of convective and large-scale precipitation, shallow convection, gravity wave drag, radiation, and boundary layer processes are included. The convective parameterization, is a version of the modified Arakawa and Schubert (1974, hereafter AS) scheme that was developed by Pan and Wu (1994). Observed precipitation is not assimilated in the NCEP-DOE; thus, all precipitation fields are based on physical parameterization and are calculated during the assimilation process. Data from the NCEP-DOE are available from 1979 to 2005, and this study uses the 6-hour daily precipitation fields (averaged to 6-hour monthly) from 1991-2000.

b. ERA-40

The ERA-40 system is based on the 1.125°x1.125° (T159, approximately 125 km), 60 level IFS CY23r4 atmospheric model

(http://www.ecmwf.int/research/ifsdocs/CY23r4/index.html). As with the NCEP-DOE, the ERA40 does not assimilate any precipitation observations. Convective precipitation is produced by the bulk mass flux scheme described in Tiedtke (1989). Once again, 6-hour monthly average precipitation fields from the ERA-40 are used from 1991-2000.

c. NARR

The final reanalysis used in this study is the relatively new, higher resolution NARR from NCEP. Reanalysis fields are available from 1979 to 2003 every 3 hours at a 32-km/45 layer resolution. Data are also used in a 6h monthly averaged form to match the other reanalyses. The NARR system utilizes a version of the Eta Model and its 3D-Var Data Assimilation System (EDAS) similar to the version that was operational in April 2003 (Mesinger et al. 2006). Differences from the operational version include a lower resolution, a different microphysics parameterization, and an increased number of observational sources. The model utilizes the Betts-Miller-Janjić convective parameterization (BMJ, Betts 1986, Janjić 1994) which is a convective adjustment type scheme. Unlike the NCEP-DOE and ERA-40, however, the NARR system does assimilate precipitation observations as latent heating profiles, as described in Lin et al. (1999). The precipitation fields, therefore, are not purely determined by the assimilated large-scale variables and the model's physical parameterizations. Precipitation data for assimilation comes from the following sources: for Mexico and Canada, a 1° rain gauge analysis is used; over the continental United States (CONUS), a 1/8° rain gauge analysis is included; the CPC merged analysis of precipitation (CMAP) global 2.5° analysis is used over oceans south of 27.5°N and land south of Mexico; no data are assimilated for oceans north of 43.5°N (Mesinger et al. 2006).

d. CPC

An objective analysis of precipitation from US station reports from the NWS/Techniques Development Laboratory as described in Higgins et al. (1996a) is used to judge the validity of precipitation in the three previously described reanalyses. This analysis is available hourly from 1948 to 2002 on a 2° latitude by 2.5° longitude grid that extends from 140°W to 60°W and 20°N to 60°N. Some uncertainty is involved in the use of this analysis because it is based on station data and, therefore, influenced by changes in the density, configuration, and temporal continuity of the observation sites, among other factors. As precipitation amounts are objectively analyzed onto grid points using a modified Cressman scheme (Cressman 1959) even if no rain gauge observations exist (for instance, over the oceans), comparisons using this information will only be done over land. To match the reanalyses, the CPC dataset is averaged to a 6-hour monthly time resolution.

Before comparison, it should be noted that the NARR and the CPC analysis are not independent datasets. They both include some of the same precipitation observations as input. Specifically, the HPD* dataset was incorporated into the CPC analysis and assimilated into the NARR over the CONUS. Although the NARR and the CPC analysis are, therefore, expected to be similar, the ingestion of precipitation data into the NARR did not guarantee that the reanalysis would match the observations after assimilation (Mesinger et al. 2006). Any divergence of the CPC from observations would be due to the objective analysis of the data., The CPC analysis is therefore used as a close and conveniently gridded approximation of the "truth".

* Hourly Precipitation Data from U.S. observing stations (Hammer and Steurer 1997)

III. Results

a. Reanalysis Precipitation

As illustrated in the left half of Fig. 1, there is a general agreement in the distribution of precipitation rate over the continental United States on an annual average basis between the NARR, ERA-40, NCEP-DOE, and the CPC dataset. Discrepancies between each of these, however, come out in the details, which are important when the data are used for weather, hydrological, and climate research. All of the datasets capture the average annual maximums in the southeast and northwest US. The NCEP-DOE, however, produces a slight excess of precipitation over the southeast, although this excess is improved compared to that in the NCEP-GR (not shown, see Kalnay et al. 1996, Trenberth and Guillemot 1998). This surplus of precipitation primarily occurs during the June-August (JJA) season, but is strong enough to show up in the annual average. The NARR agrees well with the CPC dataset over the CONUS, the slight differences are mostly due to the immense differences in resolution.

The right-hand side of Fig. 1 shows the annual cycle of precipitation for the western (center column) and eastern (right column) halves of the domain shown in the left half of Fig. 1 for 6h monthly averaged time periods over land only. The annual cycle figures were split to cover the domain from 125°W to 100°W and from 100°W to 76°W in order to remove some of the issues that arise when averaging the diurnal cycle in UTC over several time zones. Separated in this way, there are approximately two time zones per figure (a fact that should be kept in mind when interpreting them) and the areas of the country dominated by cool season and warm season precipitation are somewhat divided. Over the eastern half of the US, all of the reanalyses

correctly produce the summertime maximum in the annual cycle. It is, however, too pronounced in the NCEP-DOE (mostly because of the excessive precipitation in JJA over the Southeast). This is also the case in the ERA-40, but not to the same extent. Fall, winter, and spring average rates over the eastern half of the US are much more reasonable in all of the reanalyses, as are the distributions of precipitation during these seasons (not shown).

There are disagreements in the average US diurnal cycle over the eastern half of the country between all reanalyses. Regardless, all reanalyses, agree that the maximum in warm season precipitation occurs around 1800 UTC[†], consistent with the timing of the climatological plethora of precipitation in the Southeast. There are also issues with the diurnal cycle of precipitation throughout the cool season, but the diurnal cycle is not as amplified at this time of year, so this is not as obvious. The NARR, for all other seasons, places a strong peak in the diurnal cycle around 0600 UTC; the root of this problem will be discussed in the next section.

Over the western half of the US, the NARR and ERA-40 correctly place maximums in the annual cycle in the winter and an early evening peak in the summer, while the NCEP-DOE places the maximum in the spring (note that the winter maximum would be stronger if the coastal data were not removed by the ocean mask, not shown). The magnitude of the average wintertime precipitation is also well handled. The diurnal cycle of precipitation in the winter is problematic, but, again, it is not as amplified as the warm season diurnal cycle and, therefore, is not as obvious. Discrepancies here are largely due to differences in the timing of precipitation over Washington and Oregon. The enhanced summertime diurnal cycle in the west is well captured by the NARR and ERA-40, which both correctly place the peak time of precipitation

[†] Note that precipitation rate values are 6-hour average values; therefore, times are approximate, cover a 6-hour period, and only give a general sense of the diurnal cycle.

around 0000 UTC and minimum around 1200 UTC. The NCEP-DOE, for all seasons places the peak of the diurnal cycle around 1800 UTC.

More details on the spatial distribution of the annual cycle of precipitation rate over the US are given in Fig. 2. As with the annual average precipitation rate, this figure shows that the reanalyses and the CPC dataset are in general agreement in terms of the distribution and timing of the maximum monthly average precipitation rate. The eastern half of the US is dominated by warm season precipitation, while cool season months receive the most precipitation along the west coast. However, some disagreements are evident; especially near the transition zones between two dominant seasons of precipitation (this is especially true in the western half of the US).

A closer look will now be taken at the JJA convective season. Fig. 3 shows the maximum average 6-hour seasonal precipitation and its time of occurrence for JJA. For ease of interpretation, the time of the maximum precipitation in this figure is presented in LST instead of UTC. Also, note that the distribution of the maximum 6-hourly precipitation in this figure is similar to the distribution of the average JJA precipitation (not shown). As in the annual distribution, it is obvious here that the NCEP-DOE produces a surfeit of precipitation in the Southeast. The ERA-40 and NARR, however, well represent the maximum and timing of the maximum precipitation over the Southeast that is associated with the afternoon peak in surface heating and atmospheric instability, as measured against the CPC dataset.

The other important region of precipitation during JJA occurs over the Great Plains. Precipitation that produces the nocturnal maximum over this region in JJA is primarily produced by mesoscale convective systems (MCSs) that organize from convection initiated on the east slope of the Continental Divide typically in the late afternoon. These systems usually propagate

into the Midwest during the late evening and early morning (Carbone et al. 2002). Fig. 3 illustrates that the NARR captures this process, while the ERA-40 and NCEP-DOE generally do not[‡]. The location of the Plains maximum is displaced eastward in the ERA-40, and because the time of the maximum precipitation does not change much from west to east to indicate propagating convection, it is doubtful that the maximum encompasses the correct convective process. The NCEP-DOE does have a secondary maximum centered in eastern Colorado and a grid cell in northeast Kansas where the maximum occurs around 0000 UTC , but the overall pattern of maximum precipitation in the central portion of the US is not captured well, and the timing of the maximum precipitation in the Midwest is off by around 12h everywhere except for the aforementioned location in Kansas and an area in south-central Minnesota . Pattern correlations for the maximum amplitude and the timing of the maximum were computed for this region (87°W to 108°W and 34°N to 47°N) to quantitatively compare the amplitude and phase. The CPC, NCEP-DOE, and the ERA-40 were measured against the NARR after regridding the NARR to match the horizontal resolution of each individual dataset. Comparisons were completed using the NARR instead of the CPC dataset since the goal of this study is to examine the usefulness of the NARR relative to the other datasets. Computing correlations against the NARR also allows for a greater resolution to be used in the comparisons, as the CPC has the lowest spatial resolution of all the datasets. The correlations for the maximum amplitude in the CPC, ERA-40, and the NCEP-DOE are 0.925, 0.671, and 0.268, respectively, and for the time of the maximum, 0.686, 0.385, and 0.287. The correlation for the timing of the maximum is lower between the NARR and CPC than for the amplitude. This is likely because the transition from

[‡] To capture some detail in the NCEP-DOE southeastern US precipitation, a gray scale was used in fig. 3 that does not emphasize this important secondary maximum.

afternoon to evening precipitation occurs further west in the NARR than in the CPC. Otherwise, the correlation values reinforce the qualitative statements made above.

b. A Closer Look at NARR Precipitation

As shown above, NARR precipitation is superior to the other reanalyses examined over a domain encompassing the US, as it was designed to be. The previous results are consistent with the statement made by Mesinger et al. (2006, p. 344) that "the assimilation of precipitation during the reanalysis was found to be very successful, obtaining model precipitation quite similar to the analyzed precipitation input." To further illustrate the usefulness of the NARR, an example of an extreme event will be given to show that the NARR captures such events, even over western topography. But first, some quirks possibly caused by the model ingestion of the precipitation observations and other issues in the precipitation reanalysis are presented as a warning to potential users of this reanalysis. Since precipitation over the contiguous US in all seasons at all times appears to be very good[§] overall, but other users may draw on the data outside of the contiguous US, the information presented below is seen as completely relevant.

To start, the different precipitation observations used in creating the NARR are revealed through minimums in precipitation along the US-Canada and US-Mexico borders (see Fig. 3a, but note that these are observed more readily with finer contour intervals). More details on this discontinuity can be found in Mo et al. (2005). Other interesting features are also apparent. For instance, as shown in the rightmost panel in Fig. 1a, when averaged over a domain encompassing the eastern half of the US, the peak in the diurnal cycle does not match observations in all

[§] One exception, however, was made by West (2006) in the occasional occurrence of spurious grid-scale convection. This is not obvious in any of the climatological fields presented here though.

months. With the precipitation in a 6-hour monthly averaged form, the peak occurs at 0600 UTC, but in its original 3-hourly form, this shows up as an even stronger peak at 0900 UTC in all seasons, and is caused by exceptionally heavy precipitation at 0900 UTC in Ontario and Quebec. This is due to large precipitation systems that show up at 0900 UTC and unrealistically disappear by 1200 UTC. An example of a day where one of these systems occurs is shown in fig. 4. Observations for the nearest stations that archived observations on that day are shown in Table 1. As the locations of the stations and the observations indicate, the system that occurred around 0900 UTC on this day may or may not have existed; however, it is much like others that often occur at 0900 UTC and its evolution does not seem realistic. This problem is greatest in the fall, but it is also quite obvious in summer and spring. Systems like these show up often enough and are intense enough to also impact the frequency distribution of precipitation in individual seasons and over the whole year when a domain is used that includes part of southeast Canada (not shown). Mesinger et al. (2006, p. 357) do note that the precipitation field over Canada is "not as good as we had hoped for" due to a small number of rain gauge observations, but this is likely not a complete explanation for these events. Finding the exact cause, however, is beyond the scope of this study.

Mesinger et al. (2006) also warn that the NARR is meant to be chiefly used over land and not to be fully trusted over the oceans (especially the northern oceans) due to the lack of observations; however, one ocean oddity was noticed that is worth pointing out. Fig. 5 shows the time and magnitude of the maximum frequency of 3-hour precipitation greater than 1 mm/day (which is also representative of the spatial distribution of the average frequency of precipitation) for JJA. It shows peculiar bull's-eyes of greater frequency in the waters surrounding the southeast US coast that seem to be gridded at approximately a 2.5° interval, the

same spacing as the ingested precipitation observations. It is likely, therefore, that some part of the assimilation of the CMAP data is responsible for the bull's-eyes of precipitation that show up sporadically over these waters (e.g. see Fig. 6). These abnormally round areas of precipitation do fit to and are likely responsible for the apparently 2.5° gridded bull's-eyes on the frequency plot.

As another way to assess its utility, an example of an extreme event was chosen to see if the NARR could capture such an event. Other useful examples showing months with extreme precipitation can be found in Mesinger et al. (2006). Since it is also valuable to see how well individual precipitation episodes are portrayed, a day when flash flooding occurred in Las Vegas, Nevada was chosen for illustration. This event took place on July 8, 1999 and is described fully by Li et al. (2003). For brevity, only one period around the time of the flash flooding is considered, but as shown in Fig. 7, the 3-hour average precipitation rate from the NARR captures this event reasonably well. It portrays the intense precipitation (which is not necessarily expected from other reanalyses that do not assimilate precipitation), and the spatial pattern of the precipitation is close to what is seen in the radar imagery. As it is compared against instantaneous composite radar in this figure, an exact match is not expected (for the full evolution of the event, see Li et al. 2003). The hourly precipitation from the CPC also captures this event, but with little detail at its coarse resolution (a contour plot shows a large diamond shaped bull's-eye over most of southern Nevada, not shown). Six-hourly precipitation from the NCEP-DOE, on the other hand, does not clearly portray this event. The precipitation it produces in southern Nevada is too light by nearly an order of magnitude and is exceptionally underdone in terms of spatial coverage as well (not shown). Finally, it is also useful to mention that a few

Midwestern MCS events were examined in addition to this one and the NARR precipitation was found to compare well spatially and temporally with the actual events (not shown).

IV. Concluding Remarks

The main purpose of this note was to document several aspects of the precipitation climatology available from reanalysis datasets over the continental US. The examination of the reanalyses in Section IIIa demonstrates the superiority of the NARR in the representation of precipitation over the CONUS compared with two other widely used reanalyses. As precipitation is assimilated during the reanalysis process in the NARR, whereas it is completely parameterized in the ERA-40 and NCEP-GR, this result was anticipated. Summertime precipitation is most improved as the Plains nocturnal maximum is difficult to reproduce in models using convective parameterizations only, since parameterizations typically do not allow convection to undergo the upscale growth necessary for organization into an MCS (the primary cause of this maximum). Even if organized MCSs could be parameterized, propagation then provides another challenge (Davis et al. 2003, Bukovsky et al. 2006). For this reason, the NARR likely captures this maximum because it assimilates precipitation and not because it uses any particular parameterization.

It was also shown in Section IIIb that while the NARR replicates continental US precipitation well, care should be taken when using the precipitation analysis over the rest of the North American domain as interesting, but not necessarily valid features in other areas are found as a strong signal in some climatological fields. This note serves not only as a warning to users of the data, but also as general guidance on which aspects of the precipitation reanalyses are

most useful. Overall, as the precipitation information required becomes more detailed, the NARR becomes more useful compared to the other reanalyses, with, of course, the previously mentioned exceptions.

Acknowledgements

We would like to thank Jack Kain, Mike Baldwin, and Pete Lamb for useful discussions, as well as the three anonymous reviewers whose comments helped improve the manuscript. Support has been provided by the Gary Comer Science and Education Foundation. CPC Hourly US Precipitation data were provided by the NOAA-CIRES Climate Diagnostics Center, Boulder, Colorado, USA, from their Web site at *http://www.cdc.noaa.gov/*. ECMWF ERA-40 data were obtained through the NCAR website at *http://dss.ucar.edu/pub/era40*. NARR data were obtained from NCEP at *http://wwwt.emc.ncep.noaa.gov/mmb/rreanl/*. NCEP Reanalysis 2 data were provided by the NOAA/OAR/ESRL PSD, Boulder, CO, from their Web site at *http://www.cdc.noaa.gov*. Canadian station observations were obtained from Environment Canada's National Climate Data and Information archive at *http://www.climate.weatheroffice.ec.gc.ca*.

References

Arakawa, A. and W. H. Schubert, 1974: Interaction of a cumulus cloud ensemble with the large-scale environment, Part I. *J. Atmos. Sci.*, **31**, 674-701.

Betts, A.K., 1986: A new convective adjustment scheme. Part I: Observational and theoretical basis. *Quart. J. Roy. Meteor. Soc.*, **112**, 677-691.

Betts, A.K., 2004: Understanding hydrometeorology using global models. *Bull. Amer. Meteor. Soc.*, **85**, 1673-1688.

Betts, A.K, P. Viterbo, and E. Wood, 1998: Surface energy and water balance for the Arkansas-Red River basin from the ECMWF reanalysis. *J. Climate*, **11**, 2881-2897.

Bukovsky, M.B., J.S. Kain, M.E. Baldwin, 2006: Bowing convective systems in a popular operational model: Are they for real? *Wea. Forecasting*, **21**, 307-324.

Carbone, R.E., J. D. Tuttle, D. A. Ahijevych, and S. B. Trier, 2002: Inferences of predictability associated with warm season precipitation episodes. *J. Atmos. Sci.*, **59**, 2033-2056.

Cressman, G.P., 1959: An operational objective analysis system. *Mon. Wea. Rev.*, **87**, 367-374.

Dai, A., 1999: Recent changes in the diurnal cycle of precipitation over the United States. *Geophys. Res. Lett.*, **26**, 341-344.

Davis, C.A., K. W. Manning, R. E. Carbone, S. B. Trier, and J. D. Tuttle, 2003: Coherence of warm-season continental rainfall in numerical weather prediction models. *Mon. Wea. Rev.*, **131**, 2667-2679.

Hammer, G.R. and P.M. Steurer, 1997: Data set documentation for Hourly Precipitation Data. NOAA/NCDC TD3240 Documentation Series, Ashville, NC, 18 pp.

Hane, C.E., M.E. Baldwin, H.B. Bluestein, T.M. Crawford, and R.M. Rabin, 2001: A case study of severe storm development along a dryline within a synoptically active environment. Part I: Dryline motion and an Eta model forecast. *Mon. Wea. Rev.*, **129**, 2183-2204.

Higgins, R. W., J. E. Janowiak, and Y.-P. Yao, 1996a: A gridded hourly precipitation data base for the United States (1963-1993). NCEP/Climate Prediction Center Atlas 1, national Centers for Environmental Prediction, 46pp.

Higgins, R.W., K.C. Mo, and S.D. Schubert, 1996b: The moisture budget of the central United States in spring as evaluated in the NCEP/NCAR and the NASA/DAO reanalyses. *Mon. Wea. Rev.*, **124**, 939-963.

Janjić, Z.I., 1994: The step-mountain Eta coordinate model: Further developments of the convection, viscous sublayer, and turbulence closure schemes. *Mon. Wea. Rev.*, **122**, 927-945.

Kållberg, P., A. Simmons, S. Uppala, and M. Fuentes, 2004: The ERA-40 Archive. ERA-40 Project Report Series, Vol. 17, ECMWF, 31pp.

Kalnay, E., and Coauthors, 1996: The NCEP/NCAR 40-Year Reanalysis Project. *Bull. Amer. Meteor. Soc.*, **77,** 437–471.

Kanamitsu, M., W. Ebisuzaki, J. Woollen, S.-K. Yang, J.J. Hnilo, M. Fiorino, G.L. Potter, 2002: NCEP-DOE AMIP-II Reanalysis (R-2), *Bull. Amer. Meteor. Soc.*, **83**, 1631-1643.

Li, J., R.A. Maddox, X. Gao, S. Sorooshian, K. Hsu, 2003: A numerical investigation of storm structure and evolution during the July 1999 Las Vegas Flash Flood. *Mon. Wea. Rev.*, **131**, 2038-2059.

Lin, Y., K.E. Mitchell, E. Rogers, M.E. Baldwin, and G.I. DiMego, 1999: Test assimilations of the real-time, multi-sensor hourly precipitation analysis into the NCEP Eta model. Preprints, *8th Conf. on Mesoscale Meteorology*, Boulder, CO, Amer. Meteor. Soc., 341-344.

Mesinger, F., and Coauthors, 2006: North American Regional Reanalysis. *Bull. Amer. Meteor. Soc.*, **87**, 343-360.

Mo, K.C., M. Chelliah, M.L. Carrera, R.W. Higgins, and W. Ebisuzaki, 2005: Atmospheric moisture transport over the United States and Mexico as evaluated in the NCEP Regional Reanalysis. *J. Hydrol*., **6**, 710-728.

Pan, H.-L., and Wan-Shu Wu, 1994: Implementing a mass flux convective parameterization package for the NMC medium-range forecast model. Preprints, *10th Conf. on Numerical Weather Prediction,* Portland, OR, Amer. Meteor. Soc., 96-98.

Ruiz-Barradas, A., and S. Nigam, 2005: Warm-season rainfall variability over the US Great Plains in observations, NCEP and ERA-40 reanalyses, and NCAR and NASA atmospheric model simulations. *J. Climate*, **18**, 1808-1830.

Tiedtke, M., 1989: A comprehensive mass flux scheme for cumulus parameterization in large-scale models. *Mon. Wea. Rev.*, **117**, 1779-1800.

Trenberth, K.E., 1998: Atmospheric moisture residence times and cycling: implications for rainfall rates and climate change. *Climatic Change*, **39**, 667-694.

_____, and C.J. Guillemot, 1998: Evaluation of the atmospheric moisture and hydrological cycle in the NCEP/NCAR reanalyses. *Clim. Dyn.*, **14**, 213-231.

West, G.L., W.J. Steenburge, and W.Y.Y. Chen, 2006: Spurious grid-scale convection in the North American Regional Reanalysis. *Mon. Wea. Rev.*, submitted.

Figure Captions

Fig. 1. 1991-2000 annual average precipitation rate (left column, mm/day, contours) and 6h monthly average precipitation rate for the domain shown in the left column from 125°W to 100°W (center column, mm/day) and from 100°W to 76°W (right column, mm/day) excluding the oceans for: a) NARR, b) CPC, c) NCEP-DOE, d) ERA-40. The month of the year for the center and right columns is noted on the right-most y-axis by the first letter of each month. The divide between the two halves of the US at 100°W is indicated on the images in the left column by the heavy black line. The time key for the annual diurnal cycle figures is shown in the lower right corner in UTC. Ocean data was removed using the same 1-km resolution land/sea mask on each dataset. Note: every second horizontal grid point from the NARR dataset was used here, decreasing its resolution to 64-km, to prevent the NARR data arrays from becoming too large.

Fig. 2. 1991-2000 maximum monthly average precipitation rate (mm/day, contours) and month of maximum (vectors) from a) NARR, b) CPC, c) NCEP-DOE, d) ERA-40. Vector key inset in b). Vectors placed at the horizontal resolution of the data in all panels except panel a), where they have been "thinned". Ocean vectors in b) have been masked since the CPC data is only valid over land. Note: NARR data horizontal resolution decreased as in fig. 1.

Fig. 3. 1991-2000 JJA maximum 6h seasonal average precipitation rate (mm/day, contours) and time of maximum (vectors, LST) from a) NARR, b) CPC, c) NCEP-DOE, d) ERA-40. Vector time clock key inset in b). Vectors placed at the horizontal resolution of the data in all panels except panel a), where they have been "thinned". Ocean vectors in b) have been masked since

the CPC data is only valid over land. Note: the NARR data has been used at its full 32-km resolution and not 64-km as it was in Fig. 1.

Fig. 4. 3h average precipitation rate from the NARR for June 28, 1996. a) 0600 UTC, b) 0900 UTC, c) 1200 UTC. Symbols indicate locations of stations listed in Table 1: Geraldton, Ontario (triangle); Timmons, Ontario (diamond); North Bay, Ontario (square); Val-d'or, Quebec (circle).

Fig. 5. NARR 1991-2000 JJA maximum frequency of 3h precipitation rate greater than 1 mm/day (percent, contours) and time of maximum frequency (vectors, LST). Vector time clock key inset in figure.

Fig. 6. 3h average precipitation rate from the NARR for June 14, 1996. a) 0900 UTC, b) 1200 UTC, c) 1500 UTC.

Fig. 7. 8 July 1999 a) NARR 1800 UTC 3h average precipitation rate (mm/day), b) 1800 UTC composite radar from Fig. 7 of Li et al. (2003). Darkest grey radar echoes indicate reflectivities over 50 dBz.

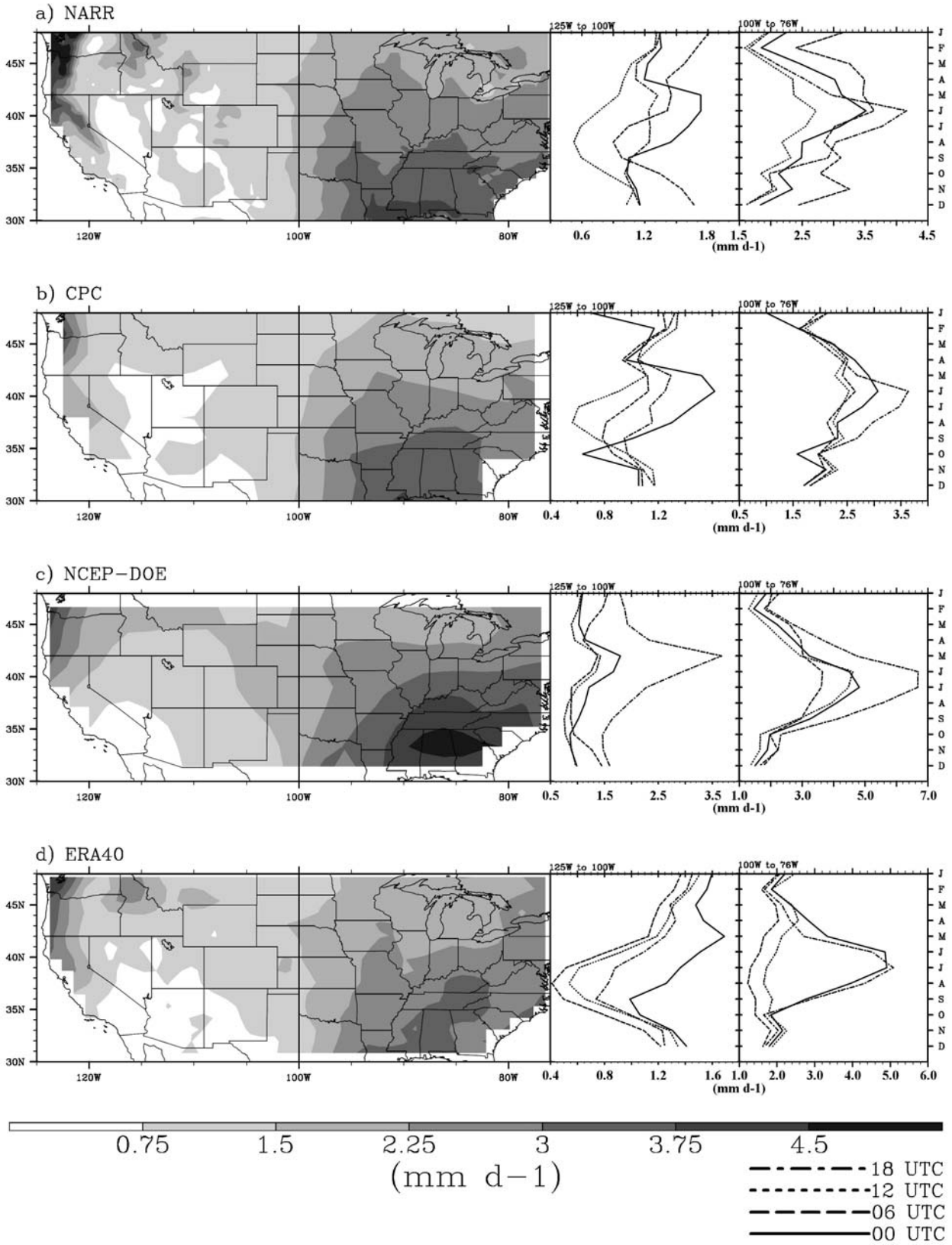
a) NARR
b) CPC
c) NCEP−DOE
d) ERA40
125W to 100W
100W to 76W
120W
100W
80W
45N
40N
35N
30N
J F M A M J J A S O N D
(mm d-1)
0.75 1.5 2.25 3 3.75 4.5
(mm d−1)
18 UTC
12 UTC
06 UTC
00 UTC

Fig. 1. 1991-2000 annual average precipitation rate (left column, mm/day, contours) and 6h monthly average precipitation rate for the domain shown in the left column from 125°W to 100°W (center column, mm/day) and from 100°W to 76°W (right column, mm/day) excluding the oceans for: a) NARR, b) CPC, c) NCEP-DOE, d) ERA-40. The month of the year for the center and right columns is noted on the right-most y-axis by the first letter of each month. The divide between the two halves of the US at 100°W is indicated on the images in the left column by the heavy black line. The time key for the annual diurnal cycle figures is shown in the lower right corner in UTC. Ocean data was removed using the same 1-km resolution land/sea mask on each dataset. Note: every second horizontal grid point from the NARR dataset was used here, decreasing its resolution to 64-km, to prevent the NARR data arrays from becoming too large.

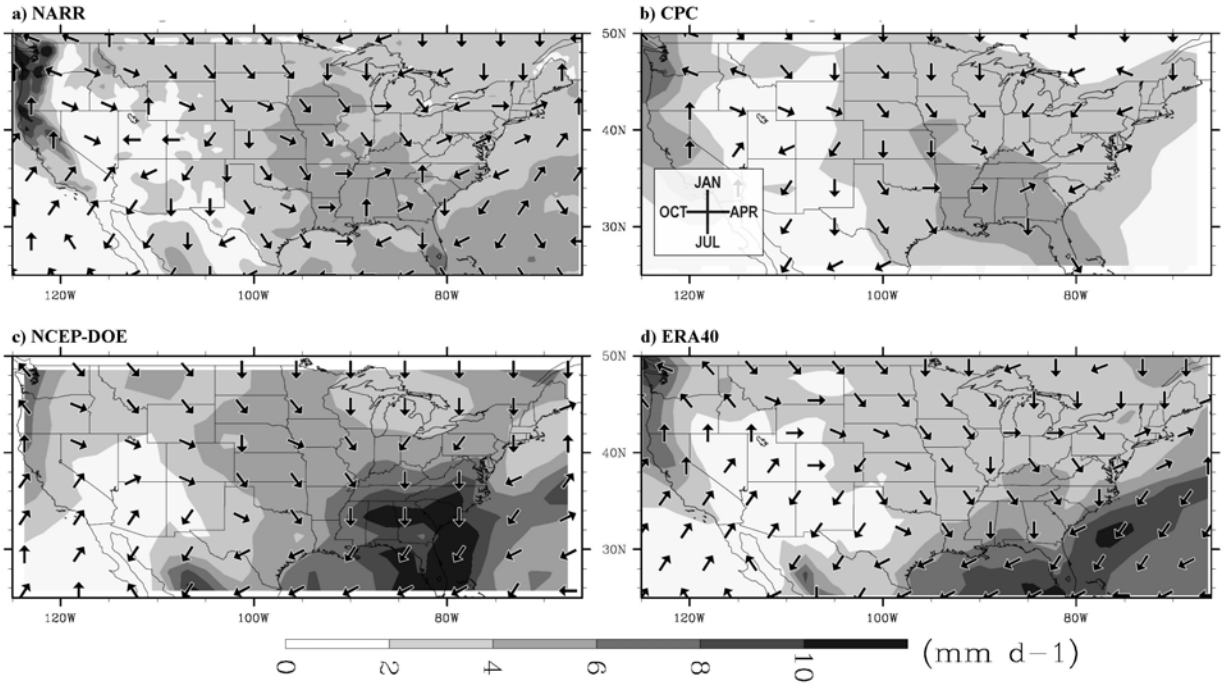

Fig. 2. 1991-2000 maximum monthly average precipitation rate (mm/day, contours) and month of maximum (vectors) from a) NARR, b) CPC, c) NCEP-DOE, d) ERA-40. Vector key inset in b). Vectors placed at the horizontal resolution of the data in all panels except panel a), where they have been "thinned". Ocean vectors in b) have been masked since the CPC data is only valid over land. Note: NARR data horizontal resolution decreased as in fig. 1.

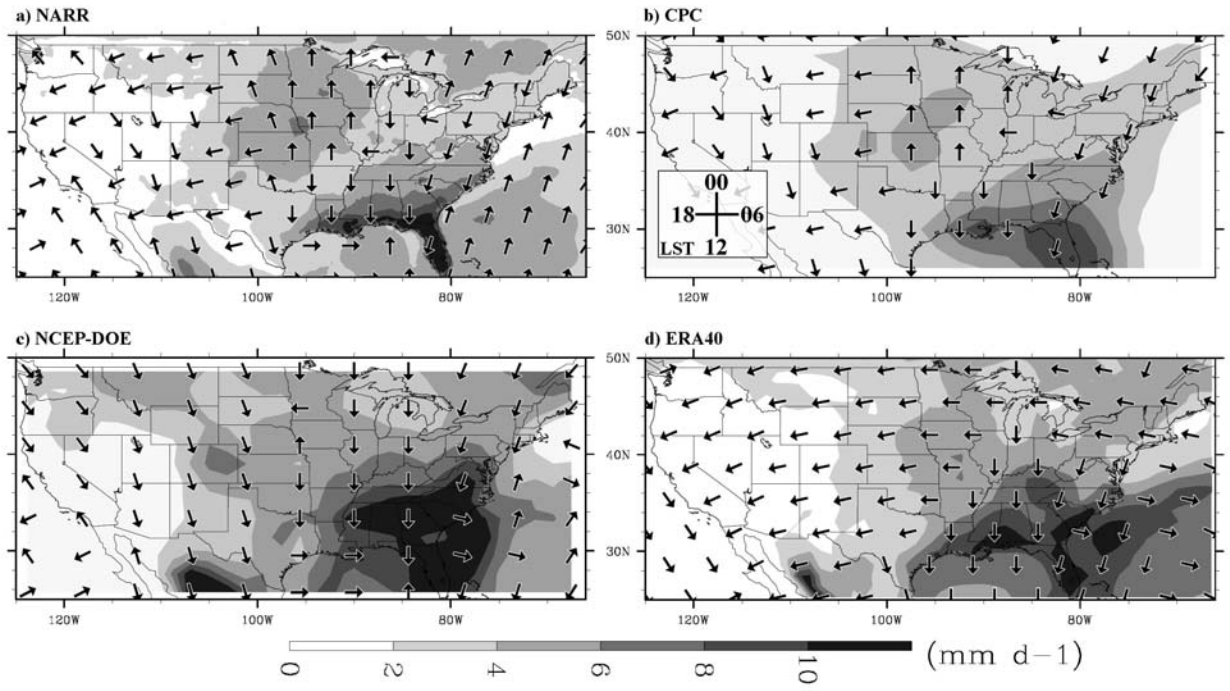

Fig. 3. 1991-2000 JJA maximum 6h seasonal average precipitation rate (mm/day, contours) and time of maximum (vectors, LST) from a) NARR, b) CPC, c) NCEP-DOE, d) ERA-40. Vector time clock key inset in b). Vectors placed at the horizontal resolution of the data in all panels except panel a), where they have been "thinned". Ocean vectors in b) have been masked since the CPC data is only valid over land. Note: the NARR data has been used at its full 32-km resolution and not 64-km as it was in Fig. 1.

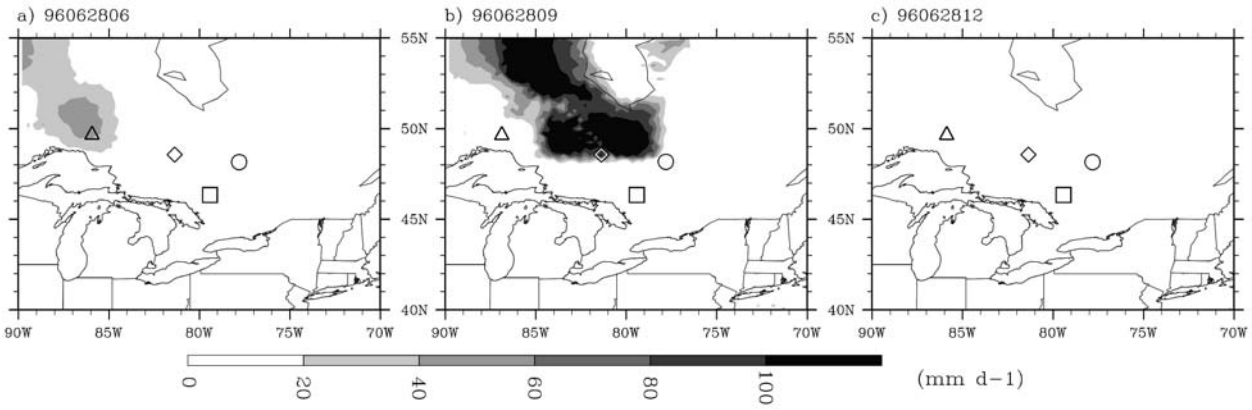

Fig. 4. 3h average precipitation rate from the NARR for June 28, 1996. a) 0600 UTC, b) 0900 UTC, c) 1200 UTC. Symbols indicate locations of stations listed in Table 1: Geraldton, Ontario (triangle); Timmons, Ontario (diamond); North Bay, Ontario (square); Val-d'or, Quebec (circle).

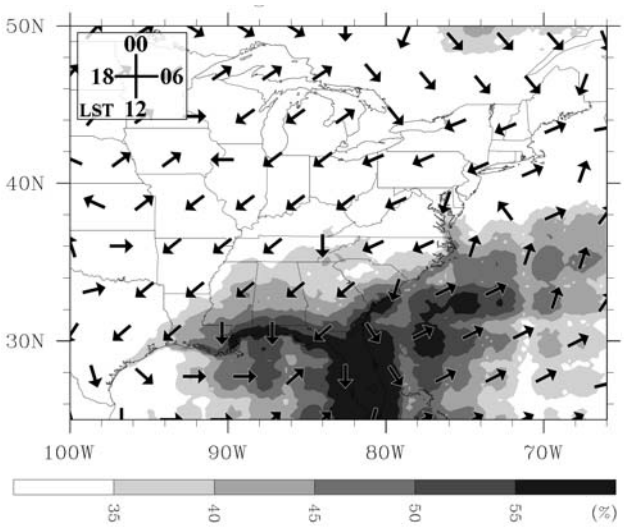

Fig. 5. NARR 1991-2000 JJA maximum frequency of 3h precipitation rate greater than 1 mm/day (percent, contours) and time of maximum frequency (vectors, LST). Vector time clock key inset in figure.

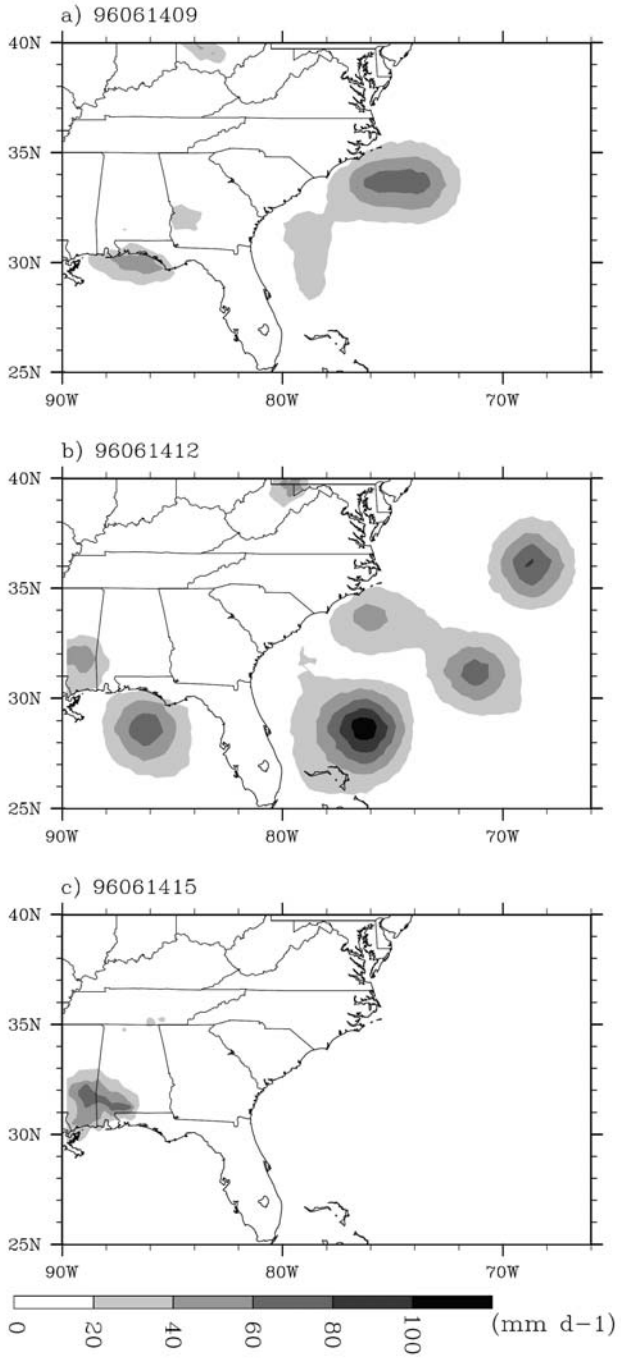

Fig. 6. 3h average precipitation rate from the NARR for June 14, 1996. a) 0900 UTC, b) 1200 UTC, c) 1500 UTC.

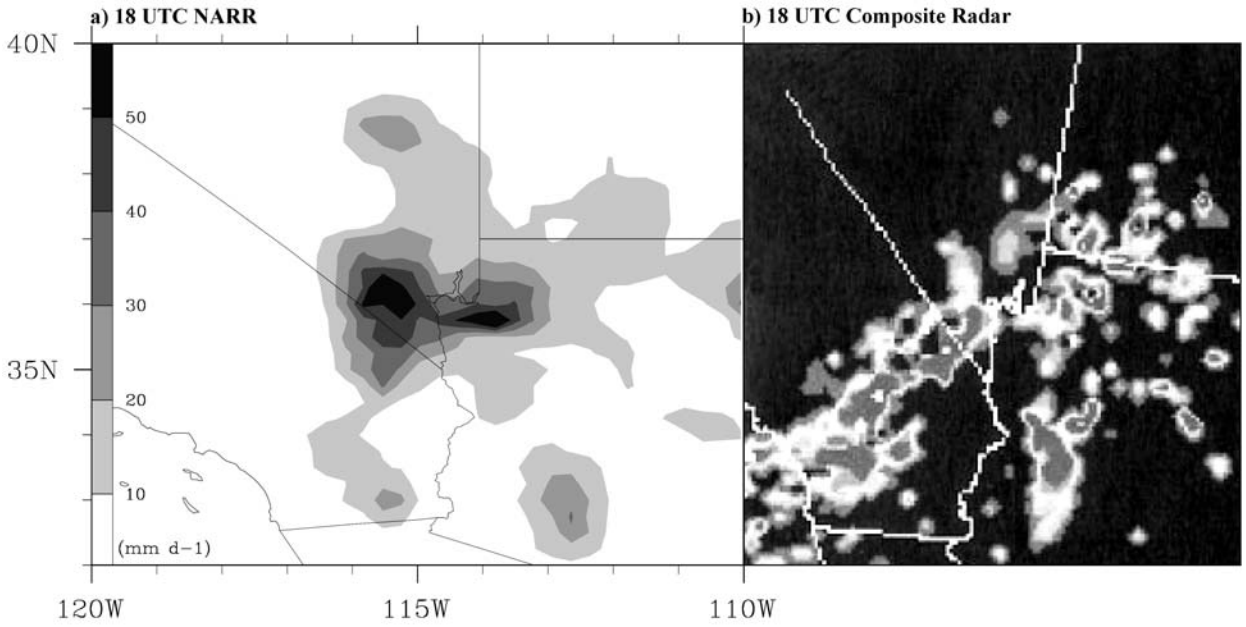

Fig. 7. 8 July 1999 a) NARR 1800 UTC 3h average precipitation rate (mm/day), b) 1800 UTC composite radar from Fig. 7 of Li et al. (2003). Darkest grey radar echoes indicate reflectivities over 50 dBz.

Table 1. Observations from 28 June 1996 for the four stations shown in Fig. 4. Times where observations are not available are indicated as n/a.

Time (UTC)	Geraldton (triangle)	Timmons (diamond)	North Bay (square)	Val-D'or (circle)
0300	Mostly Cloudy	Cloudy	Mostly Cloudy	n/a
0400	Cloudy	Cloudy	Mostly Cloudy	n/a
0500	Cloudy	Cloudy	Mainly Clear	n/a
0600	Cloudy	Cloudy	Mainly Clear	n/a
0700	Thunderstorms	Cloudy	Mostly Cloudy	n/a
0800	Thunderstorms	Cloudy	Mostly Cloudy	n/a
0900	Thunderstorms	Cloudy	Mostly Cloudy	Mostly Cloudy
1000	Thunderstorms	Cloudy	Cloudy	Mostly Cloudy
1100	Thunderstorms	Mostly Cloudy	Cloudy	Mostly Cloudy
1200	Thunderstorms	Mostly Cloudy	n/a	Mostly Cloudy
1300	Rain Showers	Cloudy	n/a	Cloudy
1400	Cloudy	Cloudy	Mostly Cloudy	Cloudy
1500	Thunderstorms	Cloudy	Cloudy	Cloudy